

Layered ACO-OFDM for intensity-modulated direct-detection optical wireless transmission

Qi Wang,¹ Chen Qian,¹ Xuhan Guo,² Zhaocheng Wang,^{1,*} David G. Cunningham,³ and Ian H. White²

¹*Tsinghua National Laboratory for Information Science and Technology (TNList), Department of Electronic Engineering, Tsinghua University, Beijing 100084, China*

²*Centre for Photonic Systems, Electrical Engineering Division, Department of Engineering, University of Cambridge, 9 J J Thomson Avenue, Cambridge CB3 0FA, UK*

³*Avago Technologies, Framlingham Technology Centre, Framlingham, Suffolk, IP13 9EZ, UK*

[*zcwang@tsinghua.edu.cn](mailto:zcwang@tsinghua.edu.cn)

Abstract: Layered asymmetrically clipped optical orthogonal frequency division multiplexing (ACO-OFDM) with high spectral efficiency is proposed in this paper for optical wireless transmission employing intensity modulation with direct detection. In contrast to the conventional ACO-OFDM, which only utilizes odd subcarriers for modulation, leading to an obvious spectral efficiency loss, in layered ACO-OFDM, the subcarriers are divided into different layers and modulated by different kinds of ACO-OFDM, which are combined for simultaneous transmission. In this way, more subcarriers are used for data transmission and the spectral efficiency is improved. An iterative receiver is also proposed for layered ACO-OFDM, where the negative clipping distortion of each layer is subtracted once it is detected so that the signals from different layers can be recovered. Theoretical analysis shows that the proposed scheme can improve the spectral efficiency by up to 2 times compared with conventional ACO-OFDM approaches with the same modulation order. Meanwhile, simulation results confirm a considerable signal-to-noise ratio gain over ACO-OFDM at the same spectral efficiency.

© 2015 Optical Society of America

OCIS codes: (060.0060) Fiber optics and optical communications; (060.2605) Free-space optical communication; (060.4510) Optical communications.

References and links

1. L. Hanzo, H. Haas, S. Imre, D. C. O'Brien, M. Rupp, and L. Gyongyosi, "Wireless myths, realities, and futures: from 3G/4G to optical and quantum wireless," *Proc. IEEE* **100**, 1853–1888 (2012).
2. A. Jovicic, J. Li, and T. Richardson, "Visible light communication: opportunities, challenges and the path to market," *IEEE Commun. Magazine* **51**(12), 26–32 (2013).
3. J. Armstrong, "OFDM for optical communications," *J. Lightwave Technol.* **27**(3), 189–204 (2009).
4. R. Zhang and L. Hanzo, "Multi-layer modulation for intensity-modulated direct-detection optical OFDM," *J. Opt. Commun. Netw.* **5**(12), 1402–1412 (2013).
5. A. M. Khalid, G. Cossu, R. Corsini, P. Choudhury, and E. Ciaramella, "1-Gb/s transmission over a phosphorescent white LED by using rate-adaptive discrete multitone modulation," *IEEE Photon. J.* **4**(5), 1465–1473 (2012).
6. G. Cossu, A. M. Khalid, P. Choudhury, R. Corsini, and E. Ciaramella, "3.4 Gbit/s visible optical wireless transmission based on RGB LED," *Opt. Express* **20**(26), B501–B506 (2012).
7. G. Cossu, A. Wajahat, R. Corsini, and E. Ciaramella, "5.6 Gbit/s downlink and 1.5 Gbit/s uplink optical wireless transmission at indoor distances (≥ 1.5 m)," in *Proceedings of ECOC*, 1–3 (2014).

8. D. Tsonev, H. Chun, S. Rajbhandari, J. J. D. McKendry, S. Videv, E. Gu, M. Haji, S. Watson, A. E. Kelly, G. Faulkner, M. D. Dawson, H. Haas, and D. O'Brien, "A 3-Gb/s single-LED OFDM-based wireless VLC link using a Gallium Nitride μ LED," *IEEE Photon. Technol. Lett.* **26**(7), 637–640 (2014).
9. J. M. Kahn and J. R. Barry, "Wireless infrared communications," *Proc. IEEE* **85**(2), 265–298 (1997).
10. J. B. Carruthers and J. M. Kahn, "Multiple-subcarrier modulation for nondirected wireless infrared communication," *IEEE J. Sel. Areas Commun.* **14**(3), 538–546 (1996).
11. J. Armstrong and B. J. C. Schmidt, "Comparison of asymmetrically clipped optical OFDM and DC-biased optical OFDM in AWGN," *IEEE Commun. Lett.* **12**(5), 343–345 (2008).
12. J. Armstrong and A. J. Lowery, "Power efficient optical OFDM," *Electron. Lett.* **42**(6), 370–372 (2006).
13. S. C. J. Lee, S. Randel, F. Breyer, and A. M. J. Koonen, "PAM-DMT for intensity-modulated and direct-detection optical communication systems," *IEEE Photon. Technol. Lett.* **21**(23), 1749–1751 (2009).
14. S. D. Dissanayake, K. Panta and J. Armstrong, "A novel technique to simultaneously transmit ACO-OFDM and DCO-OFDM in IM/DD systems," in *Proceedings of the IEEE Globecom Workshops*, 782–786 (2011).
15. S. D. Dissanayake and J. Armstrong, "Comparison of ACO-OFDM, DCO-OFDM and ADO-OFDM in IM/DD systems," *J. Lightwave Technol.* **31**(7), 1063–1072 (2013).
16. B. Ranjha and M. Kavehrad, "Hybrid asymmetrically clipped OFDM-based IM/DD optical wireless system," *J. Opt. Commun. Netw.* **6**(4), 387–396 (2014).
17. R. Mesleh, H. Elgala, and H. Haas, "LED nonlinearity mitigation techniques in optical wireless OFDM communication systems," *J. Opt. Commun. Netw.* **4**(11), 865–875 (2012).
18. L. N. Peng, S. Haese, and M. Helard, "Frequency domain LED compensation for nonlinearity mitigation in DMT systems," *IEEE Photon. Technol. Lett.* **25**(20), 2022–2025 (2013).
19. A. V. Oppenheim, W. S. Ronald, and R. B. John, *Discrete-Time Signal Processing*, 3rd ed. (Prentice-Hall, 1999).
20. X. Li, J. Vucic, V. Jungnickel, and J. Armstrong, "On the capacity of intensity-modulated direct-detection systems and the information rate of ACO-OFDM for indoor optical wireless applications," *IEEE Trans. Commun.* **60**(3), 799–809 (2012).

1. Introduction

Motivated by the dramatic development of light emitting diode (LED) technologies as well as the scarce spectrum of the radio frequency, optical wireless communication (OWC) has gained increasing attention from both of academia and industry. It has been considered as a promising complementary technique to radio frequency counterpart due to its distinct advantages such as license-free spectrum, high data rate, low power consumption and high privacy protection [1, 2]. Recently, orthogonal frequency division multiplexing (OFDM) has also been employed in OWC systems because of its inherent resistance to inter symbol interference (ISI), high spectral efficiency, and simple one-tap equalization [3, 4], whereby gigabit/s point-to-point optical wireless transmission rates have been reported in [5–8]. Since the state-of-the-art work usually focuses on point-to-point optical wireless links, the same scenario is considered throughout this paper.

In OWC systems, intensity modulation with direct detection (IM/DD) is commonly used where the transmitted electrical signal is modulated onto the instantaneous power of the optical emitter [9]. Therefore, the transmitted signal has to be real-valued and non-negative. To generate real OFDM signals, Hermitian symmetry should be imposed on the OFDM subcarriers, and only half of the subcarriers are available for modulation [3]. Generally, there are two strategies to obtain unipolar time-domain signals, namely, the biasing-based strategy and the clipping-based strategy. In the biasing-based strategy, the signal is forced to be non-negative by a DC bias. This is called DC-biased optical OFDM (DCO-OFDM) [10] and is inefficient in terms of optical power since the DC bias does not carry any information [11]. In the clipping-based strategy such as asymmetrically clipped optical OFDM (ACO-OFDM) and pulse-amplitude-modulated discrete multitone (PAM-DMT), the negative part of the output signals are directly clipped based on their antisymmetric characteristics [12, 13]. In ACO-OFDM, only the odd subcarriers are used for modulation. The output signal can be directly clipped at zero without information loss since the clipping distortion only falls on the even subcarriers [12]. PAM-DMT only modulates the imaginary part of each subcarrier and the clipping distortion only falls on the real part of the same subcarrier [13]. However, clipping-based strategy only utilizes half of

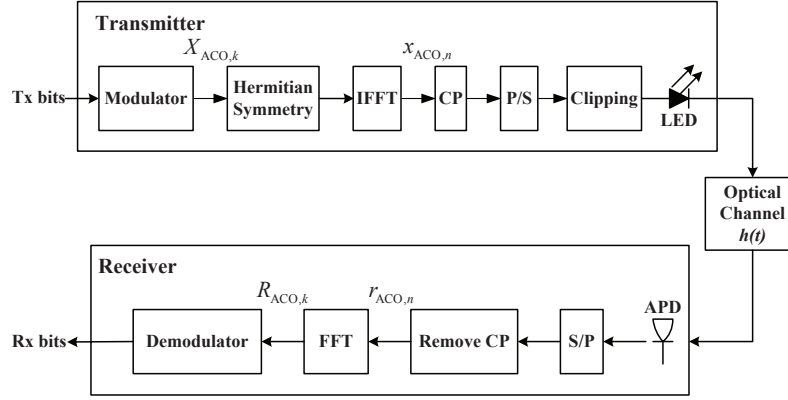


Fig. 1. IM/DD optical wireless transmission system using ACO-OFDM.

the resources in the frequency domain, leading to a spectral efficiency loss.

Several schemes have been proposed to improve the spectral efficiency of ACO-OFDM. In [14], asymmetrically clipped DC biased optical OFDM (ADO-OFDM) is proposed to apply DCO-OFDM on the even subcarriers, which is also inefficient in terms of power since DC bias is still unavoidable [15]. A hybrid ACO-OFDM (HACO-OFDM) scheme is proposed in [16], where PAM-DMT signals using even subcarriers are combined with ACO-OFDM for simultaneous transmission and DC bias is not required. However, the real part of even subcarriers is unmodulated in HACO-OFDM, which is still unable to exploit all the resources in the frequency domain.

In this paper, a spectrally efficient layered ACO-OFDM scheme is proposed for IM/DD optical wireless transmission, where different layers of ACO-OFDM are combined for simultaneous transmission. More specifically, the subcarriers are divided into different layers, modulated by different sizes of ACO-OFDM, and then combined for simultaneous transmission. An iterative receiver is also proposed for layered ACO-OFDM, where the clipping distortion of each layer is subtracted once it is detected so that the signals from different layers could be recovered. Performance analysis shows that the proposed scheme can improve the spectral efficiency by up to 2 times compared with conventional ACO-OFDM with the same modulation order. Meanwhile, simulation results also demonstrate significant signal-to-noise ratio (SNR) gain over ACO-OFDM with the same spectral efficiency.

The remainder of this paper is organized as follows. In Section 2, the conventional ACO-OFDM is presented, while in Section 3, our proposed layered ACO-OFDM and its transceiver are described. In Section 4, the performance of the proposed layered ACO-OFDM is compared to its conventional counterpart, while the conclusions are drawn in Section 5.

2. ACO-OFDM for IM/DD optical wireless transmission system

A typical IM/DD optical wireless transmission system using ACO-OFDM with N subcarriers is depicted in Fig. 1. The transmitted bit stream is mapped onto the complex-valued symbols, X_k , $k = 0, 1, \dots, N-1$, according to the chosen modulation scheme, such as PAM or quadrature amplitude modulation (QAM). Hermitian symmetry is imposed on the OFDM subcarriers to guarantee that the time-domain signals are real-valued, which means that $X_k = X_{N-k}^*$, $k = 1, 2, \dots, N/2 - 1$. Only odd subcarriers are modulated to make sure that the time-domain signals could be directly clipped at zero. The frequency-domain ACO-OFDM signals are written

as follows,

$$\mathbf{X} = [0, X_1, 0, X_3, \dots, X_{N/2-1}, 0, X_{N/2-1}^*, \dots, X_1^*]. \quad (1)$$

The time-domain ACO-OFDM signal is obtained by the inverse fast Fourier transform (IFFT) as [3]

$$x_{\text{ACO},n} = \frac{1}{\sqrt{N}} \sum_{k=0}^{N-1} X_k \exp\left(j \frac{2\pi}{N} nk\right), n = 0, 1, \dots, N-1, \quad (2)$$

which follows a half-wave symmetry as

$$x_{\text{ACO},n} = -x_{\text{ACO},n+N/2}, n = 0, 1, \dots, N/2-1. \quad (3)$$

Therefore, the negative part can be clipped without any loss of information:

$$[x_{\text{ACO},n}]_c = x_{\text{ACO},n} + i_{\text{ACO},n} = \begin{cases} x_{\text{ACO},n}, & x_{\text{ACO},n} \geq 0; \\ 0, & x_{\text{ACO},n} < 0, \end{cases} \quad (4)$$

for $n = 0, 1, \dots, N-1$, where $i_{\text{ACO},n}$ denotes the negative clipping distortion of ACO-OFDM.

After IFFT operation, a cyclic prefix (CP) is added at the beginning of each time-domain OFDM symbol to eliminate the ISI at the receiver. Afterwards, the signal is parallel to serial (P/S) converted into a single signal stream, which is then clipped at zero and used for modulating the LEDs. LED nonlinearity is a challenge for optical wireless transmission systems, which degrades its performance. Several algorithms have been proposed to mitigate the effect of nonlinearity in either time or frequency domain, and the performance degradation will be negligible when the signal is within the limit of these compensation techniques [17, 18]. Therefore, LED nonlinearity is not considered in this paper.

At the receiver, the optical signal is detected by avalanche photodiode (APD) and converted to the electronic signal. It has been proven in [12] that the negative clipping distortion only falls on the even subcarriers when transformed to the frequency domain, which is orthogonal to the transmitted data on the odd subcarriers. Thus, after serial-to-parallel (S/P) conversion and CP removal, the transmitted signal on the odd subcarriers can be recovered by using a simple FFT operation at the receiver.

3. Proposed layered ACO-OFDM

As stated above, although the conventional ACO-OFDM scheme is simple and straightforward, it only utilizes half of the available subcarriers, which results in an obvious spectral efficiency loss. To further improve the spectral efficiency, we propose a layered ACO-OFDM to occupy more available subcarriers, where asymmetric clipping could still be used in each layer and DC bias is not required. The following notations are employed throughout this paper. L -layer ACO-OFDM refers to a layered ACO-OFDM with L layers, and Layer l ACO-OFDM denotes the l -th layer in layered ACO-OFDM.

3.1. Transmitter

The time-domain signals of conventional ACO-OFDM are rewritten as $[x_{\text{ACO},n}^{(1)}]_c, n = 0, 1, \dots, N-1$, which are denoted as Layer 1 ACO-OFDM in our proposed scheme and the superscript represents the layer index. Note that only the odd subcarriers are utilized in Layer 1 ACO-OFDM.

Further, if we consider an OFDM symbol in which only even subcarriers are modulated, we have

$$\begin{aligned}
 x_n &= \frac{1}{\sqrt{N}} \sum_{k=0}^{N/2-1} X_{2k} \exp \left(j \frac{2\pi}{N} n \cdot 2k \right) \\
 &= \frac{\sqrt{2}}{2} \frac{1}{\sqrt{N/2}} \sum_{k'=0}^{N/2-1} X_{k'}^{(2)} \exp \left(j \frac{2\pi}{N/2} nk' \right) \\
 &= \frac{\sqrt{2}}{2} x_{\text{mod}(n, N/2)}^{(2)}, \quad n = 0, 1, \dots, N-1,
 \end{aligned} \tag{5}$$

where $x_n^{(2)}$ denotes the $N/2$ -point IFFT result of $X_{k'}^{(2)}$ and $\text{mod}(\cdot, N)$ represents the modulo N operator. It can be seen that x_n is periodic and can be obtained with the $N/2$ -length signal $x_n^{(2)}$. If we only utilize the subcarriers with odd indexes of $X_{k'}^{(2)}$, i.e., $X_{2(2k+1)}$, $k = 0, 1, \dots, N/4 - 1$, the time-domain signal $x_n^{(2)}$, $n = 0, 1, \dots, N/2 - 1$ also follows a half-wave symmetry as

$$x_{\text{ACO},n}^{(2)} = -x_{\text{ACO},n+N/4}^{(2)}, \quad n = 0, 1, \dots, N/4 - 1, \tag{6}$$

which could be clipped at zero without any information loss as in Eq. (4). After asymmetric clipping, we denote the generated signals $[x_{\text{ACO},n}^{(2)}]_c$ as *Layer 2 ACO-OFDM*, where we have $[x_{\text{ACO},n}^{(2)}]_c = [x_{\text{ACO}, \text{mod}(n, N/2)}^{(2)}]_c$, $n = 0, 1, \dots, N-1$. In a similar manner to the conventional ACO-OFDM, the negative clipping distortion of $[x_{\text{ACO},n}^{(2)}]_c$ only falls on the subcarriers with even indexes of $X_{k'}^{(2)}$, $k = 0, 1, \dots, N/2 - 1$, which corresponds to the $4k$ -th ($k = 0, 1, \dots, N/4 - 1$) subcarriers in the conventional ACO-OFDM. Therefore, we could obtain the other ACO-OFDM signals generated by $N/2$ -point IFFT and half of the even subcarriers could be used. Both the signals and clipping distortion of Layer 2 ACO-OFDM only fall on the even subcarriers and do not contaminate the Layer 1 ACO-OFDM signals. Therefore, we could transmit Layer 1 and Layer 2 ACO-OFDM signals simultaneously and $3/4$ of all the subcarriers are used for modulation, improving the spectral efficiency of conventional scheme by 50%.

In Layer 2 ACO-OFDM, half of the even subcarriers are modulated, i.e. $N/4$ subcarriers. The $4k$ -th ($k = 0, 1, \dots, N/4 - 1$) subcarriers remains unoccupied, which can be used to further improve the spectral efficiency. Similar to the previous derivation, we define the *Layer l ACO-OFDM* ($0 < l < \log_2 N$) as follows. We consider an OFDM symbol in which only the $2^{l-1}k$ -th ($k = 0, 1, \dots, N/2^{l-1} - 1$) subcarriers are modulated, then we have

$$\begin{aligned}
 x_n &= \frac{1}{\sqrt{N}} \sum_{k=0}^{N/2^{l-1}-1} X_{2^{l-1}k} \exp \left(j \frac{2\pi}{N} n \cdot 2^{l-1}k \right) \\
 &= \frac{1}{\sqrt{2^{l-1}}} \frac{1}{\sqrt{N/2^{l-1}}} \sum_{k'=0}^{N/2^{l-1}-1} X_{k'}^{(l)} \exp \left(j \frac{2\pi}{N/2^{l-1}} nk' \right) \\
 &= \frac{1}{\sqrt{2^{l-1}}} x_{\text{mod}(n, N/2^{l-1})}^{(l)}, \quad n = 0, 1, \dots, N-1,
 \end{aligned} \tag{7}$$

where $x_n^{(l)}$ denotes the $N/2^{l-1}$ -point IFFT result of $X_{k'}^{(l)}$. It can be seen that x_n is also periodic and can be obtained with the $N/2^{l-1}$ -length signal $x_n^{(l)}$. The Layer l ACO-OFDM signals $[x_{\text{ACO},n}^{(l)}]_c$ could be generated by modulating the subcarriers with odd indexes of $X_{k'}^{(l)}$ and $N/2^l$

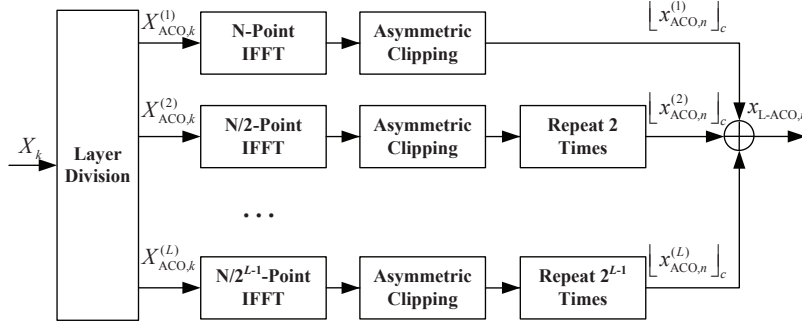


Fig. 2. Block diagram of layered ACO-OFDM transmitter with L layers.

subcarriers are utilized, where we have $\lfloor x_{\text{ACO},n}^{(l)} \rfloor_c = \lfloor x_{\text{ACO}, \bmod(n, N/2^{l-1})}^{(l)} \rfloor_c$, $n = 0, 1, \dots, N-1$.

Both the signals and clipping distortion of $\lfloor x_{\text{ACO},n}^{(l)} \rfloor_c$ only fall on the down-sampled subcarriers $X_k^{(l)}$, i.e., the $2^{l-1}k$ -th ($k = 0, 1, \dots, N/2^{l-1} - 1$) subcarriers of the original ACO-OFDM signals. Therefore, different layers of ACO-OFDM signals could be generated and the signals and clipping distortion of the Layer l ACO-OFDM are orthogonal to that of Layer $1 \sim l-1$ ACO-OFDM.

In the proposed layered ACO-OFDM scheme, different layers of ACO-OFDM are combined in the time domain for simultaneous transmission. The time-domain layered ACO-OFDM signals with L layers are written as

$$x_{\text{L-ACO},n} = \sum_{l=1}^L \lfloor x_{\text{ACO},n}^{(l)} \rfloor_c = \sum_{l=1}^L \left(x_{\text{ACO},n}^{(l)} + i_{\text{ACO},n}^{(l)} \right), n = 0, 1, \dots, N-1, \quad (8)$$

where $x_{\text{ACO},n}^{(l)}$ and $i_{\text{ACO},n}^{(l)}$ denote the unclipped signal and the negative clipping distortion of Layer l ACO-OFDM, respectively. The number of occupied subcarriers in the layered ACO-OFDM can be calculated by

$$N_{\text{L-ACO}} = \sum_{l=1}^L N/2^l = (1 - 1/2^L)N, \quad (9)$$

which is $(2 - 1/2^{L-1})$ times of conventional ACO-OFDM. When we use the maximum number of layers $L = \log_2 N - 1$, the spectral efficiency of layered ACO-OFDM would be $(2 - 4/N)$ times of conventional ACO-OFDM, which converges to 2 when N is large.

A simple block diagram of layered ACO-OFDM transmitter is shown in Fig. 2, where the modulator, Hermitian symmetry, CP insertion and P/S operations are omitted. After bit-to-symbol modulation, the modulated symbol stream is firstly divided into L streams for layered transmission. In the Layer l ACO-OFDM, only the $2^{l-1}(2k+1)$ -th ($k = 0, 1, \dots, N/2^l - 1$) subcarriers are modulated, which are orthogonal to all the other layers. Due to the periodicity of the time-domain signals as shown in Eq. (7), the Layer l ACO-OFDM could be simply implemented by $N/2^{l-1}$ -point IFFT and the $N/2^{l-1}$ -length signals are then repeated 2^{l-1} times to obtain the N -length OFDM signals. Afterwards, the time-domain signals from L layers of ACO-OFDM are combined for simultaneous transmission. Since asymmetric clipping is performed in all the L layers, the combined layered ACO-OFDM signals are also non-negative and no DC bias is required for obtaining unipolar time-domain signals.

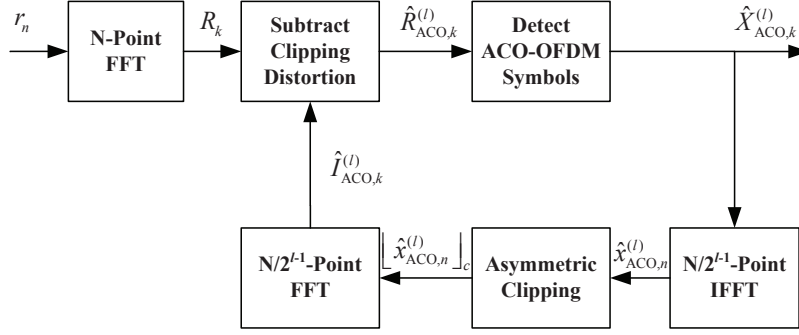


Fig. 3. Block diagram of iterative receiver for layered ACO-OFDM.

3.2. Receiver

At the receiver, the shot noise and thermal noise is usually modeled as additive white Gaussian noise (AWGN) [13–16], and the received signal is given by

$$r_n = h_n x_{L-ACO,n} + w_n, n = 0, 1, \dots, N-1, \quad (10)$$

where w_n and h_n denote the samples of AWGN and channel state information, respectively. The received signal is fed to the FFT block and the frequency-domain symbols are generated as $R_k = H_k X_{L-ACO,k} + W_k$ for $k = 0, 1, \dots, N-1$.

In layered ACO-OFDM, different layers utilize different subcarriers, which are orthogonal in the frequency domain. However, due to the asymmetric clipping operation at the transmitter, the negative clipping distortion falls on the even subcarriers in each layer and distorts the higher layers. For Layer l ACO-OFDM, the negative clipping distortion falls on the $2^{l-1}(2k+1)$ -th ($k = 0, 1, \dots, N/2^l - 1$) subcarriers, where the Layer $l+1$ ACO-OFDM are modulated. Therefore, the symbols in higher layers could be recovered only after the negative clipping distortion from their corresponding lower layers has been removed. In this subsection, we propose an iterative receiver for layered ACO-OFDM.

A simple block diagram of the iterative receiver for layered ACO-OFDM is shown in Fig. 3, where the S/P and CP removal operations are also omitted. For Layer l ACO-OFDM, we denote the received frequency-domain symbol and negative clipping distortion as $\hat{R}_{ACO,k}^{(l)}$ and $\hat{I}_{ACO,k}^{(l)}$, where we have $k = 0, 1, \dots, N/2^{l-1} - 1$. For the Layer 1 ACO-OFDM, the transmitted symbols could be directly detected by using the odd subcarriers of R_k , we have $\hat{R}_{ACO,k}^{(1)} = R_k$ and

$$\hat{X}_{ACO,k}^{(1)} = \arg \min_{X \in \mathcal{S}_{ACO}} |H_k X - 2\hat{R}_{ACO,k}^{(1)}|, k = 1, 3, \dots, N/2 - 1, \quad (11)$$

where \mathcal{S}_{ACO} denotes the constellation set of ACO-OFDM. The factor of 2 in Eq. (11) is due to the fact that the clipping operation reduces the power of ACO-OFDM symbols in the odd subcarriers by half.

The estimated time-domain Layer 1 ACO-OFDM signal $\left[\hat{x}_{ACO,n}^{(1)}\right]_c$ could be regenerated by $\hat{X}_{ACO,k}^{(1)}$, and the frequency-domain negative clipping distortion of Layer 1 ACO-OFDM $\hat{I}_{ACO,k}^{(1)}$ could also be estimated by FFT of $\left[\hat{x}_{ACO,n}^{(1)}\right]_c$. After subtracting $\hat{I}_{ACO,k}^{(1)}$ from the received frequency-domain symbols on the even subcarriers, the Layer 2 ACO-OFDM symbols could be detected.

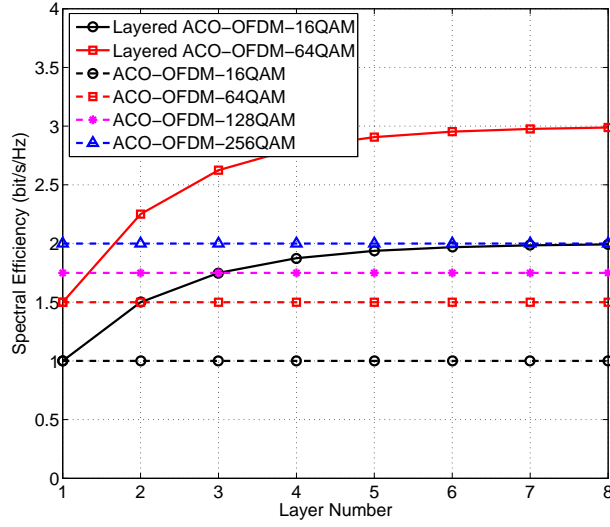


Fig. 4. Spectral efficiency comparison of layered ACO-OFDM and its conventional counterpart.

For Layer l ($l > 1$) ACO-OFDM, the negative clipping distortion from layer $1 \sim l-1$ ACO-OFDM should be removed and the received frequency-domain symbols can be calculated by

$$\begin{aligned}\hat{R}_{\text{ACO},k}^{(l)} &= R_{2^{l-1}k} - H_{2^{l-1}k} \sum_{m=1}^{l-1} \hat{r}_{\text{ACO},2^{l-m}k}^{(m)} \\ &= \hat{R}_{\text{ACO},2k}^{(l-1)} - H_{2^{l-1}k} \hat{r}_{\text{ACO},2k}^{(l-1)}, \quad k = 0, 1, \dots, N/2^{l-1} - 1,\end{aligned}\quad (12)$$

where only one subtraction operation is required for each symbol. Similar to Eq. (11), the transmitted symbols in Layer l ACO-OFDM can be detected by

$$\hat{X}_{\text{ACO},k}^{(l)} = \arg \min_{X \in \mathcal{S}_{\text{ACO}}} |H_{2^{l-1}k} X - 2\hat{R}_{\text{ACO},k}^{(l)}|, \quad k = 1, 3, \dots, N/2^{l-1} - 1. \quad (13)$$

Therefore, the layered ACO-OFDM could be detected in an iterative way as shown in Fig. 3.

3.3. Performance evaluation

The spectral efficiencies of the layered ACO-OFDM and the conventional ACO-OFDM are compared in Fig. 4, where the length of CP is omitted. It can be seen that the proposed scheme improves the spectral efficiency of ACO-OFDM significantly when the same modulation order is used. The spectral efficiency of layered ACO-OFDM improves when the layer number increases and it converges to twice of conventional ACO-OFDM when the layer number is large enough, so that capacity-approaching transmission could be achieved [20]. Even with a small number of layers such as $L = 4$, the spectral efficiency improvement is still considerable, i.e., 87.5%. When we use 2-layer and 3-layer ACO-OFDM with 16QAM, they achieve the same spectral efficiency as ACO-OFDM with 64QAM and 128QAM. Therefore, lower modulation order could be adopted in layered ACO-OFDM to achieve the same spectral efficiency as ACO-OFDM, which has lower signal-to-noise ratio (SNR) requirement at the receiver.

To guarantee that the information bits in different layers have similar performance, the modulation scheme and average power of modulated subcarriers should be the same in each layer. In Layer 1 ACO-OFDM, the symbols are directly detected with the received signals and they are only distorted by the noise at the receiver. In other layers, however, the symbols are also distorted by the estimation error of the negative clipping distortion in previous layers, which would degrade their performance. Fortunately, when the SNR increases, the estimation of negative clipping distortion becomes more accurate and the performance of the other layers converges to that of Layer 1, which will be verified by simulations.

3.4. Complexity analysis

The complexity of a layered ACO-OFDM transceiver is analyzed in this section. At the transmitter, only one N -point IFFT is required in conventional ACO-OFDM and its complexity can be written as $O(N \log_2(N))$ [19]. In layered ACO-OFDM with L layers, however, L different sizes of IFFT blocks are employed, and the total computational complexity would increase to $\sum_{l=1}^L O(N/2^{l-1} \log_2(N/2^{l-1})) \approx (2 - 1/2^{L-1}) O(N \log_2(N))$. Therefore, the computational complexity of layered ACO-OFDM transmitter is less than twice of the conventional ACO-OFDM transmitter and this complexity increase is the same as the spectral efficiency improvement. Since the L layers are calculated at the same time, there is no more latency compared with conventional ACO-OFDM.

At the receiver, the computational complexity of conventional ACO-OFDM is also $O(N \log_2(N))$ since only one N -point FFT is utilized. In layered ACO-OFDM with L layers, the computational complexity would be $O(N \log_2(N)) + 2 \sum_{l=1}^{L-1} O(N/2^{l-1} \log_2(N/2^{l-1})) \approx (5 - 1/2^{L-3}) O(N \log_2(N))$, which is less than 5 times of the conventional ACO-OFDM receiver. In hardware implementation, the complexity of layered ACO-OFDM receiver is only twice of the conventional one since we could reuse the same N -point FFT/IFFT block. With the assumption that N is the power of 2, for the sequence with length $N/2^l$, a length N sequence can be obtained by zero-padding and the same N -point FFT/IFFT block can be reused. The iterative structure also leads to extra latency in the proposed layered ACO-OFDM receiver. Fortunately, when the number of layers increases, the sizes of FFT/IFFT used in the iterative receiver decrease exponentially and the latency of the iterative receiver is also $(5 - 1/2^{L-3})$ times of the conventional ACO-OFDM receiver, which is acceptable considering the improvement of spectral efficiency. Since different systems have various requirements, there should be a tradeoff between complexity and latency in practical scenarios.

4. Numerical results

The bit error rate (BER) performance of the proposed layered ACO-OFDM is evaluated by back-to-back simulations in terms of normalized optical bit energy to noise power ratio $E_{b(opt)}/N_0$, where the average optical power is set to unity [11]. The number of IFFT used at the transmitter is 512 and the double-sided bandwidth of the LED is assumed to be 200 MHz. The subcarriers are modulated by 16QAM in all layers, and the power of each modulated subcarriers is the same in each layer. The proposed iterative receiver is employed at the receiver. Figure 5 shows the BER performance of layered ACO-OFDM with 4 layers, where the BER in each layer of ACO-OFDM is calculated separately. It can be seen that the symbols in layered ACO-OFDM could be detected successfully with the proposed iterative receiver. For the same $E_{b(opt)}/N_0$ level, the BER increases with the layer number since the symbols in higher layers are distorted by the estimation error of the lower layers. However, as shown in Fig. 5, when $E_{b(opt)}/N_0$ increases, the estimation accuracy improves with the reduction of BER in higher

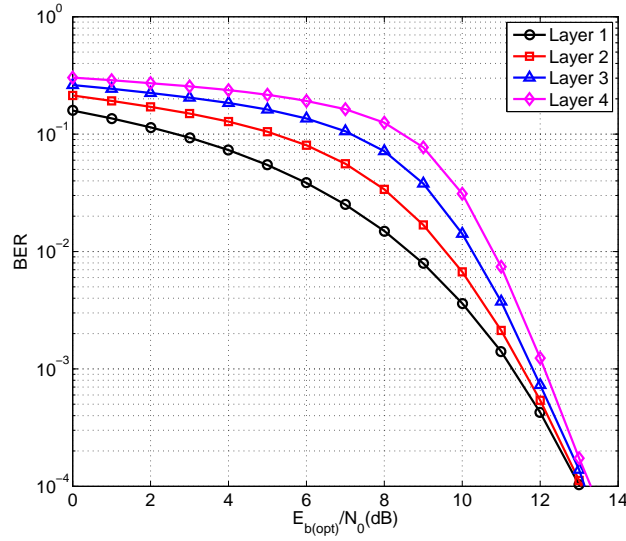


Fig. 5. BER performance of the proposed layered ACO-OFDM with 16QAM and 4 layers.

layers, and the four BER curves converge, which is also the working point for the practical system. This result also matches the performance analysis in Section 3.3.

The average BER of layered ACO-OFDM is compared with that of conventional ACO-OFDM and HACO-OFDM in Fig. 6, where BERs of all layers in layered ACO-OFDM are averaged. In layered ACO-OFDM, the subcarriers are modulated by 16QAM in all layers. The numbers of layers are set to 2, 3 and 4, and the spectral efficiencies are 1.5 bits/s/Hz, 1.75 bits/s/Hz and 1.875 bits/s/Hz, respectively. Correspondingly, the data rates of the three modulations are 300 Mbps, 350 Mbps and 375 Mbps by multiplying the bandwidth and the spectral efficiencies. Three different kinds of ACO-OFDM are used for comparison, where the odd subcarriers are modulated by 16QAM, 64QAM, and 128QAM, corresponding to the spectral efficiencies of 1 bit/s/Hz, 1.5 bits/s/Hz and 1.75 bits/s/Hz. In HACO-OFDM, the odd subcarriers are modulated by ACO-OFDM with 16QAM and 64QAM and the even subcarriers are modulated by PAM-DMT with 4PAM and 2PAM, corresponding to the spectral efficiencies of 1.5 bit/s/Hz and 1.75 bits/s/Hz. The optimal proportions of optical power for HACO-OFDM is obtained by the method in [16], and the proportions of optical power allocated to ACO-OFDM block are 0.6 and 0.85 for two different HACO-OFDM schemes.

When the same modulation orders are used, the performance of layered ACO-OFDM is worse than the conventional ACO-OFDM, which is due to the fact that the power of layered ACO-OFDM in each layer is smaller than that of the conventional ACO-OFDM since it is distributed to different layers. For example, at the BER of 10^{-4} , the performance degradations of layered ACO-OFDM-16QAM with 2, 3, and 4 layers are 1.8 dB, 2.46 dB, and 2.85 dB compared the conventional ACO-OFDM-16QAM, but the spectral efficiency is improved by 50%, 75%, and 87.5% as shown in Fig. 4.

When we compare the three schemes with the same spectral efficiency, it can be seen that the proposed ACO-OFDM significantly outperforms the conventional ACO-OFDM, and it is also better than HACO-OFDM. At the BER of 10^{-4} , the 2-layer ACO-OFDM-16QAM achieves 2.51 dB gain compared with ACO-OFDM-64QAM with the same spectral efficiency of 1.5 bits/s/Hz. Even compared with HACO-OFDM with the same spectral efficiency, the per-

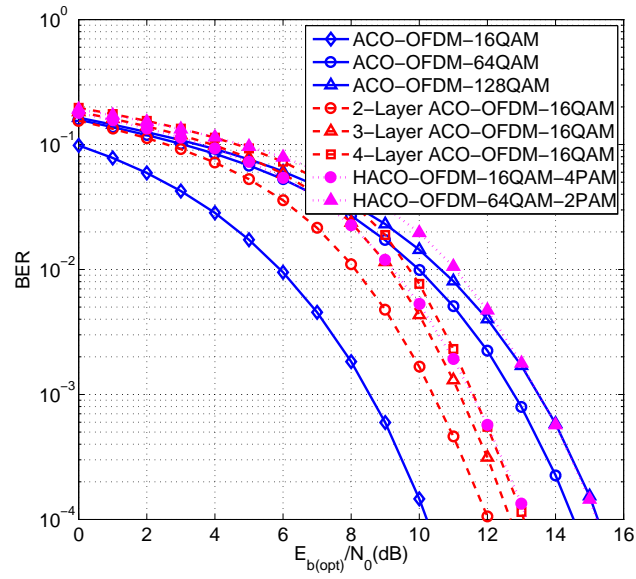


Fig. 6. BER performance comparison of the proposed layered ACO-OFDM and its conventional counterpart (optical).

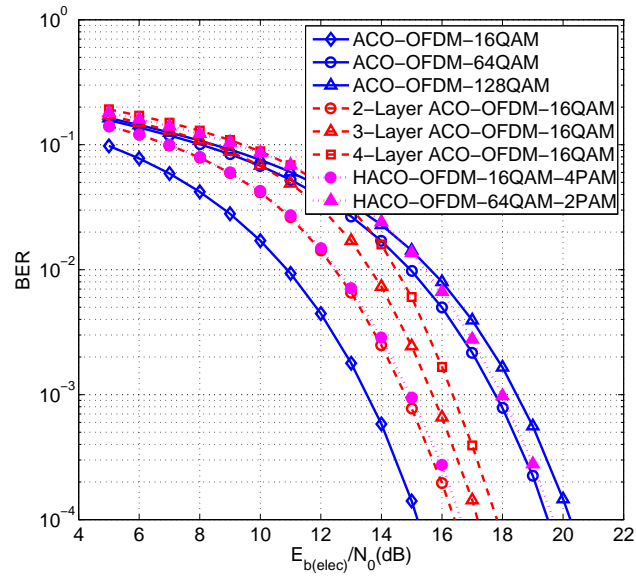


Fig. 7. BER performance comparison of the proposed layered ACO-OFDM and its conventional counterpart (electrical).

formance gain is still 1.13 dB. For the 3-layer ACO-OFDM-16QAM, it also outperforms ACO-OFDM-128QAM by 2.56 dB with the same spectral efficiency of 1.75 bits/s/Hz, while HACO-OFDM with the same spectral efficiency has almost the same performance as ACO-OFDM.

When 4-layer ACO-OFDM-16QAM is employed, which has 0.125 bits/s/Hz more spectral efficiency compared with ACO-OFDM-128QAM, the performance gain is still 2.17 dB.

The BER performance of the proposed layered ACO-OFDM is also evaluated by simulations in terms of the electrical bit energy to noise power ratio $E_{b(elec)}/N_0$, which is shown in Fig. 7. When $E_{b(elec)}/N_0$ is considered, we can see that the proposed layered ACO-OFDM scheme still outperforms conventional ACO-OFDM and HACO-OFDM approaches with the same spectral efficiency.

5. Conclusions

In this paper, a spectrally efficient layered ACO-OFDM scheme is proposed for IM/DD optical wireless transmission, where the subcarriers are divided into different layers and modulated by different sizes of ACO-OFDM, which are combined and radiated at the same time. At the receiver, the symbols in different layers are decoded in an iterative way. Compared with the conventional scheme, the layered ACO-OFDM scheme improves the spectral efficiency by utilizing more subcarriers and up to 2 times improvement can be achieved. Simulation results demonstrate that the layered ACO-OFDM also obtains considerable SNR gains when the spectral efficiency is the same as its conventional counterparts.

Acknowledgment

This work was supported by National Key Basic Research Program of China (Grant No. 2013CB329203), National Nature Science Foundation of China (Grant No. 61271266), Shenzhen Visible Light Communication System Key Laboratory (ZDSYS20140512114229398) and Shenzhen Peacock Plan (No. 1108170036003286).